Journal of Magnetic Resonance **152,** 179–184 (2001)
doi:10.1006/jmre.2001.2386, available online at http://www.idealibrary.com on IDEAL®

S^3E-E.COSY Methods for the Measurement of ^{19}F Associated Scalar and Dipolar Coupling Constants

Burkhard Luy,* Joseph J. Barchi, Jr.,† and John P. Marino*,[1]

*Center for Advanced Research in Biotechnology, University of Maryland and the National Institute for Standards and Technology, 9600 Gudelsky Drive Rockville, Maryland 20850; and †Laboratory of Medicinal Chemistry, National Cancer Institute, FCRDC, Frederick, Maryland 21702

Received March 15, 2001; revised May 25, 2001; published online August 1, 2001

A ^1H–^{19}F spin state selective excitation (S^3E) pulse sequence element has been applied in combination with ^1H homonuclear mixing to create E.COSY-type experiments designed to measure scalar $J_{HF2'}$ and $J_{HH2'}$ and residual dipolar $D_{HF2'}$ and $D_{HH2'}$ couplings in 2′-deoxy-2′-fluoro-sugars. The ^1H–^{19}F S^3E pulse sequence element, which resembles a simple INEPT sequence, achieves spin-state-selective correlation between geminal ^1H–^{19}F spin pairs by linear combination of in-phase ^{19}F magnetization and anti-phase magnetization evolved from ^1H. Since the S^3E sequence converts both ^{19}F and ^1H steady-state polarization into observable coherences, an approximately twofold signal increase is observed for fully relaxed ^1H–^{19}F spin pairs with respect to a standard ^1H coupled ^{19}F 1D experiment. The improved sensitivity and resolution afforded by the use of ^1H–^{19}F S^3E E.COSY-type experiments for measuring couplings is demonstrated on the nucleoside 9-(2′,3′-dideoxy-2′-fluoro-β-D-*threo*-pentofuranosyl)adenine (β-FddA) and on a selectively 2′-fluorine labeled 21mer RNA oligonucleotide.

Key Words: **S^3E; E.COSY; fluorine; RNA; scalar couplings; residual dipolar couplings.**

INTRODUCTION

E.COSY-type (*1–3*) techniques provide a convenient way to measure scalar and dipolar couplings in macromolecules. The E.COSY method is based on the use of mixing sequences that specifically restrict the coherence transfer allowed to only correlations between connected transitions. The restricted coherence transfer results in simplified cross peak multiplet component patterns from which the magnitude and sign of the coupling constant of interest can be measured. Recently, a spin-state selective excitation (S^3E) pulse sequence element (*4–6*) was introduced which allows editing of a two-spin system into two separate subspectra corresponding to the spin-coupled nucleus being in either the α or β state. Methods that utilize the S^3E pulse sequence element within the context of E.COSY-type experiments have been described for the measurement of homonuclear J_{HH} (*4*) and heteronuclear J_{HC} and J_{HN} (*5*) couplings.

[1] To whom correspondence should be addressed. E-mail: marino@carb.nist.gov.

Here, a simple ^1H–^{19}F spin-state selective excitation (S^3E) pulse sequence element is applied in combination with homonuclear ^1H mixing schemes to generate E.COSY-type spectra which allow for the sensitive measurement of scalar $J_{HF2'}$ and $J_{HH2'}$ and residual dipolar $D_{HF2'}$ and $D_{HH2'}$ couplings in 2′-deoxy-2′-fluoro-sugars (Scheme 1). The utility of ^1H–^{19}F S^3E-E.COSY-type experiments in measuring these coupling constants is demonstrated on the nucleoside 9-(2′,3′-dideoxy-2′-fluoro-β-D-*threo*-pentofuranosyl)adenine (β-FddA) (*7*) and on a selectively 2′-fluorine labeled 21mer RNA oligonucleotide (*8*). Using ^1H–^{19}F S^3E-E.COSY-type experiments, the cross peak components generated in the two subspectra are approximately twice as sensitive as the components of the cross peak doublet generated using conventional t_1-coupled E.COSY experiments (*9*). In addition, as previously reported (*4–6*), the S^3E-E.COSY-type experiments are equivalent in resolution to standard decoupled ^1H–^{19}F correlated spectra since two subspectra are generated, each with only one of the two components of the E.COSY cross peak.

^1H–^{19}F SPIN STATE SELECTION

For the case of an isolated ^1H–^{19}F coupled spin pair, spin-state-selective excitation (S^3E) of exclusively either F_yH^β or F_yH^α coherence can be achieved using the simple INEPT-type pulse sequence shown in Fig. 1A. In this ^{19}F-detected INEPT experiment, proton steady-state magnetization H_z (at point *a* in the sequence) is transferred into the observable anti-phase operator H_zF_y or $-H_zF_y$ (at point *c* in the sequence), depending on the phase of ϕ_1. During the same INEPT period, steady-state magnetization from the heteronucleus F_z (at point *b* in the sequence) is also excited to the in-phase operator F_y, leading to the overall observable operator of $r^*F_y \pm H_zF_y$ (at point *c* in the sequence), with r being equal to the ratio γ_F/γ_H. Since ^{19}F has approximately the same gyromagnetic ratio as a proton ($\gamma_F/\gamma_H \sim 0.94$), the factor r can be estimated to be unity and the observable magnetization corresponds to F_yH^β or F_yH^α, respectively. The ^{19}F-detected S^3E experiment is demonstrated using diethyl-fluoromalonate [$HFC(COOCH_2CH_3)_2$], a molecule that contains an isolated ^1H–^{19}F coupled spin system. Depending

1090-7807/01

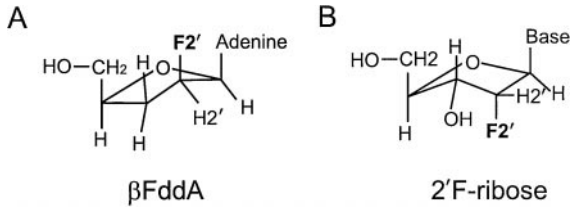

SCHEME 1. (A) Chemical structure the nucleoside 9-(2′,3′-dideoxy-2′-fluoro-β-D-*threo*-pentofuranosyl)adenine (β-FddA) and (B) 2′F-ribose. Fluorine atoms are shown in bold.

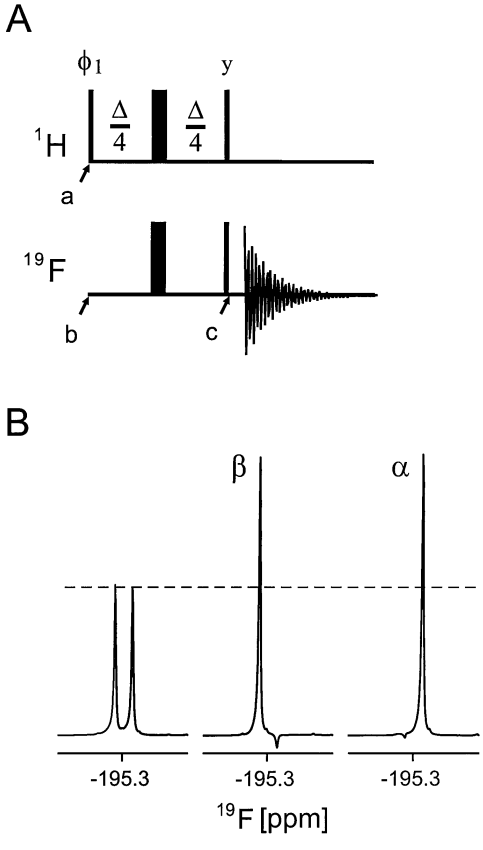

FIG. 1. (A) General pulse sequence scheme for the ^{1}H and ^{19}F excited, ^{19}F detected 1D experiment using spin-state-selective excitation (S^3E) for selection of either the α-state ($\phi_1 = -x$) or the β-state ($\phi_1 = x$). Spin-state-selective magnetization $F_y \pm F_y H_z$ (c) is obtained by the simultaneous transformation of proton magnetization (a) H_z into antiphase and excitation of ^{19}F magnetization (b) F_z. Narrow and wide vertical lines indicate 90° and 180° flip angle pulses, respectively. All pulses are applied along x unless otherwise indicated. Delay Δ is set to the geminal HF coupling, $1/J(^1\mathrm{H},^{19}\mathrm{F})$. (B) Comparison of standard 1D ^{1}H-coupled ^{19}F spectra of diethyl-fluoromalonate (*1*) with two 1D ^{19}F spectra of the same molecule acquired using the ^{1}H and ^{19}F excited, ^{19}F detected S^3E pulse scheme of Fig. 1A with ϕ_1 set either to x or $-x$ to select for the β or α state, respectively, of the proton magnetization on our Bruker DRX500 spectrometer. All spectra were collected under identical conditions with a single scan. The fluorine transmitter was centered at -195.3 ppm. A dashed line is drawn to indicate that the S^3E experiments can achieve twice the magnitude, relative to the ^{1}H-coupled ^{19}F spectra multiplet, due to equal contribution of the ^{19}F and ^{1}H nuclei in the S^3E element.

on the phase ϕ_1, either the β or the α spin state of the fluorine signal is selected (Fig. 1B). Since the observable magnetization originates equally from ^{1}H and ^{19}F, the observed multiplet component has approximately twice the intensity as in a proton-coupled ^{19}F-1D, as predicted based on the γ_F/γ_H ratio. It is also clear from the spectra in Fig. 1B that the S^3E element provides a high degree of discrimination between the two doublet states, with only very minor residual artifacts.

The extension of the S^3E INEPT-type experiment to a 2D experiment requires the addition of a back transfer of ^{19}F magnetization into observable ^{1}H magnetization. In the back transfer, special care must be taken so that the spin states are conserved. As reported earlier (*4–6*), this can be achieved by a planar mixing or sensitivity enhancement step (*10, 11*). The resulting 2D ^{1}H–^{19}F S^3E correlated experiment is shown in Fig. 2A. Depending on the phase of ϕ_1 and ϕ_2 (see Fig. 2 legend for

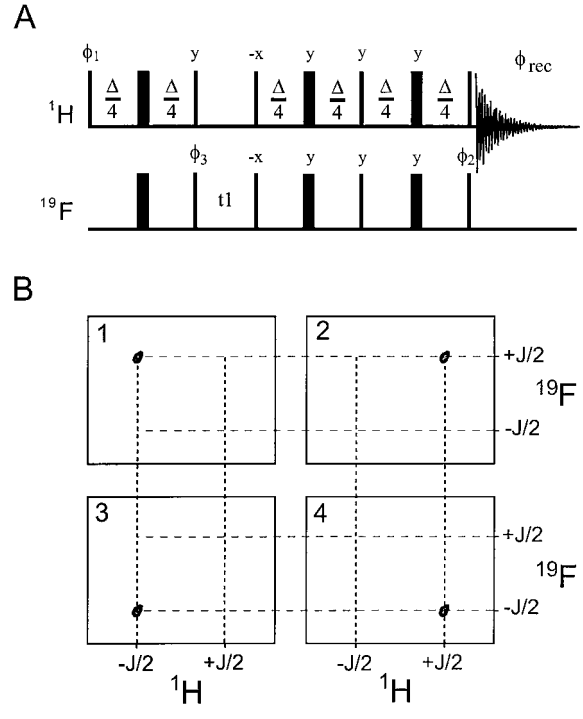

FIG. 2. (A) Pulse sequence of a ^{1}H and ^{19}F excited ^{1}H,^{19}F- S^3E HETCOR 2D experiment with ^{19}F evolution during t_1 and proton detection. After spin-state selection and ^{19}F evolution, the back transfer is achieved via a planar mixing or sensitivity enhancement building block. The (^{19}F, ^{1}H)-spin-state-selection is achieved by setting the phases on our Bruker DRX500 spectrometer according to (α, α): $\phi_1 = -x$, $\phi_2 = x$; (α, β): $\phi_1 = -x$, $\phi_2 = -x$; (β, α): $\phi_1 = x$, $\phi_2 = -x$; (β, β): $\phi_1 = x$, $\phi_2 = x$. Narrow and wide vertical lines indicate 90° and 180° flip angle pulses, respectively. All pulses are applied along x unless otherwise indicated. Delay Δ is set to the geminal HF coupling, $1/J(^1\mathrm{H},^{19}\mathrm{F})$. Quadrature detection in ω_1 was obtained by incrementing ϕ_3 according to States-TPPI. (B) 2D spectra of the four possible observable multiplets for the HF coupled spin pair of diethyl-fluoromalonate, that can be selectively measured using the ^{1}H,^{19}F HETCOR S^3E pulse scheme of Fig. 2A. The four versions of the experiment were acquired by varying the phase of ϕ_1 and ϕ_2 as mentioned above. The fluorine transmitter was centered at -195.3 ppm and the proton transmitter was centered at 5.6 ppm.

experimental details), each of the four components ($\alpha\alpha$, $\alpha\beta$, $\beta\alpha$, and $\beta\beta$) of an HF correlated cross peak can be selectively observed, as again demonstrated on diethyl-fluoromalonate (Fig. 2B).

MEASUREMENT OF COUPLINGS

The ^{1}H–^{19}F S^{3}E pulse sequence element described above can be used to construct E.COSY-type experiments for measuring scalar and residual dipolar couplings. Since subspectra are generated using the ^{1}H–^{19}F S^{3}E methods with only one component of an E.COSY doublet, this method provides an elegant way to eliminate the potential increase in overlap that may result from the generation of doublets in a standard E.COSY measurement. In addition, the use of S^{3}E to correlate ^{1}H–^{19}F coupled spins as described here also improves the signal to noise ratio of the observed cross peaks by approximately a factor of 2 relative to conventional E.COSY experiments. Figure 3 shows pulse sequences for the measurement of heteronuclear ^{1}H–^{19}F coupling constants with t_1 evolution of either the ^{19}F (A) or ^{1}H resonances (B). These sequences have been adapted from previously published experiments (*4–6*). The sequences use the ^{1}H–^{19}F S^{3}E element as a filter for ^{19}F-coupled ^{1}H resonances followed by a homonuclear mixing step in which ^{1}H magnetization is transferred to other protons so that long-range ^{1}H–^{19}F couplings can be measured. TOCSY, NOESY, and DTOCSY (i.e., transfer via residual dipolar couplings originally introduced as DCOSY (*12*)) were employed as the mixing steps in this study. In principle, however, the mixing step can be any type of homonuclear correlation experiment.

Figure 3A shows a pulse sequence for measuring ^{1}H–^{19}F couplings, which uses Z gradients for artifact suppression, while the sequence in Fig. 3B uses spin lock pulses for the same purpose. The data in this study were collected with spin-lock versions of the experiments since the ^{1}H/^{19}F dual resonance probehead used did not have the capability of applying actively shielded pulsed field gradients. The pulse sequence shown in Fig. 3C is designed for the measurement of long range ^{1}H–^{1}H couplings. In this case, after the ^{1}H–^{19}F S^{3}E filter and the homonuclear mixing step a second planar mixing period is added which selectively transfers the α/β spin state of the fluorine to the coupled proton, leading to the corresponding spin state selection for the proton–proton coupling.

In spin systems where the fluorine experiences more than one significant ^{1}H–^{19}F coupling (as is the case for β-FddA and 2′F-labeled RNA), selective 180° ^{1}H pulses can be used to refocus only the geminal H2′ proton coupled to the fluorine. The selective 180° ^{1}H pulses serve to significantly enhance the signal to noise ratio and strongly reduced lineshape artifacts that can result from imperfect refocusing of multiple J_{HF} couplings of different magnitudes. Selective 180° ^{1}H pulses can be applied to the geminal H2′ protons in 2′F-labeled sugars, since these protons are fortuitously downfield shifted into a unique chemical shift range with respect to the other sugar protons H1′, H3′, H4′, and H5′. In certain cases, however, overlap of the H1′ and H2′ chemical shift ranges in 2′F-labeled RNA samples and close proximity in chemical shift ranges of the H1′, H2′, and other ribose protons may preclude perfect selective refocusing of only H2′ protons. Selective 180° ^{1}H pulses have been implemented within the context of the pulse sequence in Fig. 3C and can also be applied in a similar fashion in place of the nonselective hard 180° ^{1}H pulses in the pulse sequences shown in Figs. 3A and 3B.

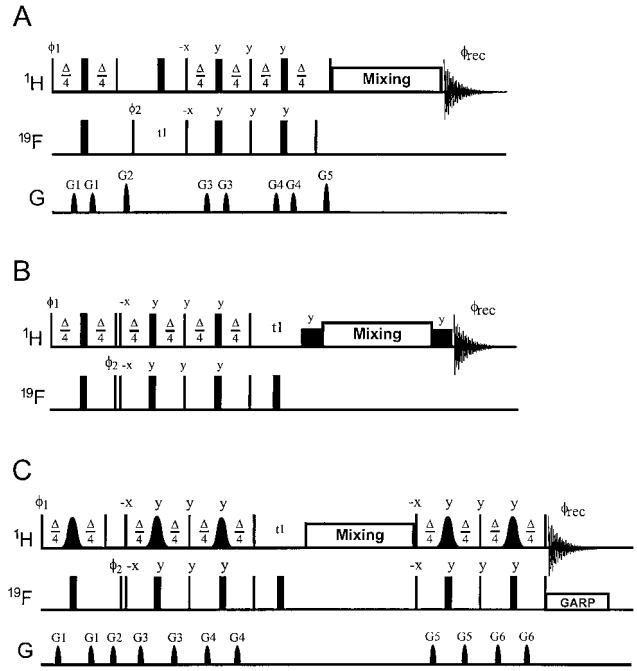

FIG. 3. S^{3}E-E.COSY-type experiments for measuring heteronuclear ^{19}F–^{1}H and homonuclear ^{1}H–^{1}H coupling constants. Sequences (A) and (B) are designed to measure heteronuclear ^{19}F–^{1}H couplings with the ω_1 dimension being either (A) ^{19}F or (B) ^{1}H. Sequence (A) shows the gradient version of the experiment while (B) uses spin lock pulses around the homonuclear mixing step for artifact suppression. Sequence (C) is designed to measure homonuclear ^{1}H–^{1}H coupling constants (*4*) and is shown as the gradient version of the experiment. In sequence C, the use of H2′-selective inversion pulses for refocusing of the protons significantly increases the signal intensity for spin systems, like 2′F-labeled sugars, where the fluorine has more than one significant ^{19}F–^{1}H coupling. These H2′-selective inversion pulses can also be applied in sequences (A) and (B) to gain improvement in signal intensity and artifact suppression. Narrow and wide vertical lines indicate 90° and 180° flip angle pulses, respectively, bell-shaped pulses indicate selective G3-inversion pulses covering the geminal bound proton region. All pulses are applied along x unless otherwise indicated. In all sequences the delay Δ is set to the geminal HF coupling, $1/J(^1\mathrm{H},^{19}\mathrm{F}) \sim 9.0$ ms. In all experiments the β- and α-state are obtained by setting the phase $\phi_1 = x$ and $\phi_1 = -x$, respectively. ^{19}F-filtering and pure phase quadrature detection was achieved by cycling $\phi_2 = \phi_{rec} = x, -x$, and according to States-TPPI.

The ^{1}H–^{19}F S^{3}E-E.COSY type experiments have been applied to β-FddA, which is labeled with a single fluorine at the 2″-proton position of the sugar ring, and to a 21mer RNA hairpin, which has been specifically labeled with fluorine at the 2′-hydroxyl position of three ribose sugars (Fig. 5A). In Fig. 4,

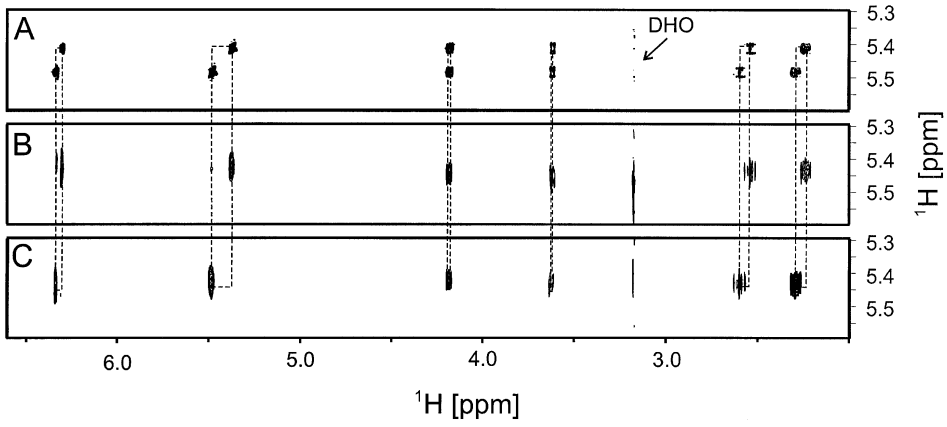

FIG. 4. (A) ^{19}F X-filtered E.COSY-TOCSY experiment and (B, C) the α and β S^{3}E E.COSY-TOCSY experiments applied to β-FddA. The DIPSI-2 sequence (*22*) was used as for the homonuclear mixing step in each experiment, with a spin-lock period of 50 ms and a 90° pulse of length 34 μs. Spectra were collected with 8 scans per t_1 increment with spectral width of 5000 Hz in ω_2 and ω_1, respectively, at 25°C on a Bruker DRX500 spectrometer equipped with a ^{1}H/^{19}F dual probe. The fluorine transmitter was centered at −188 ppm and the proton transmitter was centered at 5 ppm. For the ^{19}F X-filtered E.COSY-TOCSY experiment 4096 ($t_2^{max} = 410$ ms) and 512 ($t_1^{max} = 205$ ms) complex points in ω_2 and ω_1, respectively, were collected. For the S^{3}E E.COSY-TOCSY experiment, 4096 ($t_2^{max} =$ 410 ms) and 128 ($t_1^{max} = 51.2$ ms) complex points in ω_2 and ω_1, respectively, were collected, since there was no need to resolve a multiplet structure in t_1. The ^{19}F X-filtered E.COSY-TOCSY ran for 6 h and the S^{3}E E.COSY-TOCSY ran for 1.5 h each using a ∼5 mM sample dissolved in 99.98% DMSO-d$_7$. The 2D data were processed and plotted using standard protocols in nmrPipe (*23*).

the ^{1}H–^{19}F S^{3}E-E.COSY-TOCSY is compared to a conventional X-filtered-E.COSY-TOCSY (*13–16*). As can easily be seen, the α and β spin state selective experiments include only one part of the doublet so that the coupling can be measured using the relative chemical shift displacement of the doublet components in the two subspectra. Since the α and β spin states are in separate spectra, the number of increments in the ω_1 dimension could be significantly reduced compared to the conventional X-filtered-E.COSY-TOCSY. This reduction led to a total acquisition time of only ∼3 h for the two ^{1}H–^{19}F S^{3}E-E.COSY-TOCSY experiments together, whereas ∼6 h were needed for the conventional X-filtered-E.COSY-TOCSY. Moreover, the sensitivity of the 3 h ^{1}H–^{19}F S^{3}E-E.COSY-TOCSY experiments was still better than the longer conventional experiment. The ^{1}H–^{19}F coupling constants extracted from the spectra collected using the pulse sequences in Fig. 3A and from the experiment for measurement of ^{1}H–^{1}H couplings in Fig. 3C (spectra not shown) applied to β-FddA are given in Table 1 with a comparison to couplings measured previously by standard line-fitting of high-resolution 1D ^{1}H spectra using the program gNMR (Shorewell Scientific, Oxford, UK).

^{1}H–^{19}F coupling constants have also been measured on the 2′F-labeled R1inv hairpin using conventional X-filtered-E.COSY-NOESY (*13–16*) and ^{1}H–^{19}F S^{3}E-E.COSY-NOESY experiments (Fig. 5B). In comparing these spectra, the α and β S^{3}E spectra again showed improved signal to noise ratios relative to the conventional X-filtered experiment. For this selectively 2′F-labeled RNA, the improved resolution afforded by the S^{3}E subspectra in comparison to conventional X-filtered E.COSY spectra is not needed due to the small number of ^{19}F labels. Nevertheless, it is clear that for more extensively 2′F-labeled

TABLE 1
J_{HH} and J_{HF} Couplings Determined for β-FddA

β-FDDA	Simulated fit of 1D data	S^{3}E Measurement
2′F–H1′	16.0	15.9
2′F–H2′	54.5	54.8
2′F–H3′	28.0	28.3
2′F–H3″	27.3	27.3
2′F–H4′	n.d.	0.6
H2′–H1′	4.0	3.8
H2′–H3′	3.7	3.7
H2′–H3″	6.2	6.1

Note. n.d. = not determined by line-fitting.

TABLE 2
J_{HF} Couplings Determined for the 21mer RNA Stem-Loop

2′F-R1inv	X-filtered E.COSY-NOESY	S^{3}E-E.COSY-NOESY
2′F–H1′ U9	17.4	17.3
2′F–H2′ U9	51.5	51.6
2′F–H3′ U9	20.5	20.7
2′F–H1′ U16	14.0	14.2
2′F–H2′ U16	50.6	50.6
2′F–H3′ U16	22.8[a]	22.5[a]
2′F–H1′ U17	14.1	14.1
2′F–H2′ U17	50.5	50.3
2′F–H3′ U17	24.2[a]	24.4[a]

[a] Cross peaks show distorted line shapes because they resonate close to the residual HDO signal.

RNAs the reduction in the number of cross peaks by half in the S^{3}E subspectra will certainly give an advantage in resolution. The coupling constants derived from the conventional and S^{3}E methods applied to the 2′F-labeled R1inv hairpin are given in Table 2 for comparison. The deviations in the measured coupling constants between the different experiments are within the error of the measurements. A ^{1}H–^{19}F S^{3}E-E.COSY-DTOCSY experiment was also performed on the same RNA 21mer hairpin oriented in solution using liquid crystalline bacteriophage

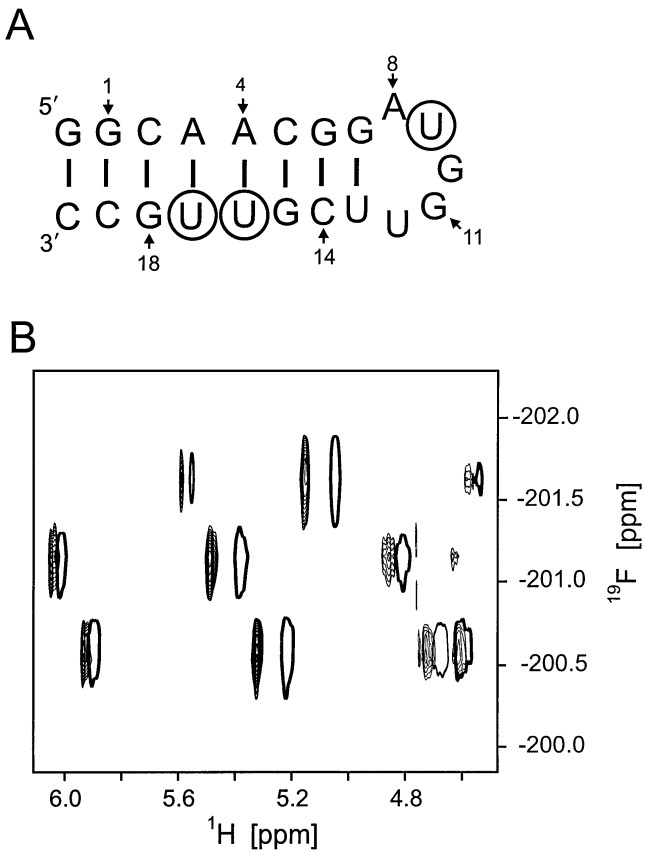

FIG. 5. (A) Schematic of the secondary structure of the 21mer R1inv RNA hairpin. Hydrogen bonded base pairs are connected by solid lines. Selectively F2′-labeled positions [U9 (loop), U16 and U17 (stem)] are circled. (B) 2D ^{19}F,^{1}H correlated spectra collected using the pulse scheme of Fig. 3A with a 400 ms NOESY as the homonuclear mixing step applied to ∼1 mM sample of the 21mer RNA hairpin in 1 mM Cacodylate [pH 6.5], 25 mM NaCl in 99.96% D_2O. Spectra were collected with 4096 ($t_2^{max} = 410$ ms) and 32 ($t_1^{max} = 13.6$ ms) complex points in ω_2 and ω_1, respectively, at 25°C on a Bruker DRX500 spectrometer equipped with a ^{1}H/^{19}F dual probe. The fluorine transmitter was centered at −201 ppm and the proton transmitter was centered on residual HDO signal (4.75 ppm). 256 scans per t_1 increment were collected with spectral widths of 5000 and 2350 Hz in ω_2 and ω_1, respectively. Each experiment was run for 10 h. The 2D data were processed and plotted using standard protocols in nmrPipe (*23*). The observed cross peaks from the H^β state version of the experiment are shown with multiple black contour lines and cross peaks from the H^α state version of the experiment are shown as a single black contour line. From the separation between the cross peaks observed in the two experiments, ^{19}F–^{1}H scalar coupling constants could be determined and are listed in Table 2.

TABLE 3
Sum of D_{HF} and J_{HF} Couplings Determined for the 21mer RNA Stem-Loop

Cross Peak	X-filtered-E.COSY-DTOCSY w Pf1	S^{3}E-E.COSY-DTOCSY w Pf1
2′F-U9–H1′-U9	13.0	13.2
2′F-U9–H2′-U9	54.0	53.6
2′F-U16–H1′-U16	8.5	8.5
2′F-U16–H2′-U16	53.7	53.6
2′F-U16–H6-U17	0.5	0.7
2′F-U17–H1′-U17	7.9	7.9
2′F-U17–H2′-U17	54.0	54.5
2′F-U17–H8-G18	1.1	1.0

Pf1 media (*17*, *18*), with a Pf1 concentration of 12 mg/ml. In this experiment, the MOCCA-XY16 multiple pulse sequence (*19*), which has special coherence transfer properties with respect to dipolar coupled spin systems (*20*, *21*), was used to efficiently transfer the ^{19}F coupled H2′ proton magnetization to other proton resonances via ^{1}H–^{1}H residual dipolar couplings. The sum of scalar and residual dipolar couplings measured in this experiment are given in Table 3. The comparison with the couplings extracted from the X-filtered E.COSY-DTOCSY experiment (*16*) shows the reliability of the S^{3}E measurements even if J evolution delays are slightly off due to the additional ^{1}H–^{19}F residual dipolar couplings.

SUMMARY

In this study, ^{1}H–^{19}F S^{3}E pulse sequence elements were used to improve the sensitivity and resolution of E.COSY-type methods designed to measure scalar $J_{HF2'}$ and $J_{HH2'}$ and residual dipolar $D_{HF2'}$ and $D_{HH2'}$ coupling constants. The ^{1}H–^{19}F S^{3}E pulse sequence element achieves an improvement of approximately a factor of two in signal to noise when compared to conventional E.COSY experiments, where the initial magnetization of only one of the nuclei is selected. In addition, the ^{1}H–^{19}F S^{3}E method generates two subspectra that are of equivalent resolution to a normal decoupled ^{1}H–^{19}F correlated spectra. These ^{1}H–^{19}F S^{3}E methods therefore provide a more efficient way to measure ^{19}F-associated couplings in 2′F-labeled nucleosides, nucleotides and oligonucleotides.

ACKNOWLEDGMENTS

This work was supported by NIH Grant (GM 59107-01) to J.P.M. B.L. acknowledges a Feodor Lynen fellowship from the AvH-Stiftung. We thank F. Song (CARB) for synthesis of ^{19}F labeled RNA, A. Pardi (University of Colorado) for providing Pf1 starter cultures, and F. Kramer and S. J. Glaser (TU-München) for making the MOCCA sequences available prior to publication and for interesting discussions. Certain commercial equipment, instruments, and materials are identified in this paper in order to specify the experimental procedure. Such identification does not imply recommendation or endorsement by the National Institute of Standards and Technology, nor does it imply that the material or equipment identified is necessarily the best available for the purpose.

REFERENCES

1. C. Griesinger, O. W. Sørensen, and R. R. Ernst, Two-dimensional correlation of connected NMR transitions, *J. Am. Chem. Soc.* **107,** 6394–6396 (1985).
2. C. Griesinger, O. W. Sørensen, and R. R. Ernst, Correlation of connected transitions by two-dimensional NMR spectroscopy, *J. Chem. Phys.* **85,** 6837–6852 (1986).
3. C. Griesinger, O. W. Sørensen, and R. R. Ernst, Practical aspects of the E.COSY technique. Measurement of scalar spin–spin coupling constants in peptides, *J. Magn. Reson.* **75,** 474–492 (1987).
4. A. Meissner, J. O. Duus, and O. W. Sørensen, Spin-state-selective excitation. Application for E.COSY-type measurement of J(HH) coupling constants, *J. Magn. Reson.* **128**(1), 92–97 (1997).
5. M. D. Sorensen, A. Meissner, and O. W. Sørensen, Spin-state-selective coherence transfer via intermediate states of two-spin coherence in IS spin systems: Application to E.COSY-type measurement of J coupling constants, *J. Biomol. NMR.* **10**(2), 181–186 (1997).
6. A. Meissner, T. Schulte-Herbrüggen, and O. W. Sørensen, Spin-state-selective polarization or excitation for simultaneous E.COSY-type measurement of (3)J(C′,H-alpha) and 3J(H-N,H-alpha) coupling constants with enhanced sensitivity and resolution in multidimensional NMR spectroscopy of C-13,N-15-labeled proteins, *J. Am. Chem. Soc.* **120**(15), 3803–3804 (1998).
7. M. A. Siddiqui, V. E. Marquez, J. S. Driscoll, and J. J. Barchi, A diastereoselective synthesis of (S,S)-alpha-fluoro-2,2-dimethyl-1,3-dioxolane-4-propanoic acid methyl-ester, a key intermediate for the preparation of anti-HIV effective fluorodideoxynucleosides, *Tetrahedron Lett.* **35**(20), 3263–3266 (1994).
8. Y. Eguchi and J. Tomizawa, Complexes formed by complementary RNA stem-loops: Their formations, structures and interaction with ColE1 Rom protein, *J. Mol. Biol.* **220,** 831–842 (1991).
9. B. Reif, V. Wittmann, H. Schwalbe, C. Griesinger, K. Worner, K. JahnHofmann, J. W. Engels, and W. Bermel, Structural comparison of oligoribonucleotides and their 2′-deoxy-2′-fluoro analogs by heteronuclear NMR spectroscopy, *Helv. Chim. Acta.* **80**(6), 1952–1971 (1997).
10. W. Willker, and D. Leibfritz, Accurate measurement of homonuclear coupling-constants using JHH-TOCSY, *J. Magn. Reson.* **99**(2), 421–425 (1992).
11. T. Schulteherbruggen, Z. L. Madi, O. W. Sørensen, and R. R. Ernst, Reduction of multiplet complexity in COSY-type NMR-spectra—The bilinear and planar COSY experiments, *Mol. Phys.* **72**(4), 847–871 (1991).
12. M. R. Hansen, M. Rance, and A. Pardi, Observation of long-range H-1-H-1 distances in solution by dipolar coupling interactions, *J. Am. Chem. Soc.* **120**(43), 11,210–11,211 (1998).
13. A. S. Edison, W. M. Westler, and J. L. Markley, Elucidation of amino acid spin systems in proteins and determination of heteronuclear coupling constants by carbon–proton–proton three-dimensional NMR, *J. Magn. Reson.* **92,** 434–438 (1991).
14. J. V. Hines, G. Varani, S. M. Landry, and I. J. Tinoco, The stereospecific assignment of H5′ and H5″ in RNA using the sign of two-bond carbon–proton scalar couplings, *J. Am. Chem. Soc.* **115**(23), 11,002–11,003 (1993).
15. J. V. Hines, S. M. Landry, G. Varani, and I. Tinoco, Jr., Carbon–proton scalar couplings in RNA: 3D heteronuclear and 2D isotope-edited NMR of a 13C-labeled extra-stable hairpin, *J. Am. Chem. Soc.* **116**, 5823–5831 (1994).
16. B. Luy and J. P. Marino, Measurement and application of 1H-19F dipolar couplings in the structure determination of 2′-fluorolabeled RNA, *J. Biomol. NMR* **20**(1), 39–47 (2001).
17. M. R. Hansen, L. Mueller, and A. Pardi, Tunable alignment of macromolecules by filamentous phage yields dipolar coupling interactions, *Nat. Struct. Biol.* **5**(12), 1065–1074 (1998).
18. M. R. Hansen, P. Hanson, and A. Pardi, Filamentous bacteriophage for aligning RNA, DNA, and proteins for measurement of nuclear magnetic resonance dipolar coupling interactions, *RNA–Ligand Interactions Pt A.* **317,** 220–240 (2000).
19. F. Kramer, W. Peti, C. Griesinger, and S. J. Glaser, Optimized homonuclear Carr–Purcell-type dipolar mixing sequences, *J. Magn. Reson.* **149**(1), 58–66 (2001).
20. B. Luy and S. J. Glaser, Analytical polarization and coherence transfer functions for three dipolar coupled spins 1/2, *J. Magn. Reson.* **142**(2), 280–287 (2000).
21. B. Luy and S. J. Glaser, Superposition of scalar and residual dipolar couplings: Analytical transfer functions for three spins 1/2 under cylindrical mixing conditions, *J. Magn. Reson.* **148**(1), 169–181 (2001).
22. A. J. Shaka, C. J. Lee, and A. Pines, Iterative schemes for bilinear operators; Application to spin decoupling, *J. Magn. Reson.* **77,** 274–293 (1988).
23. F. Delaglio, S. Grzesiek, G. W. Vuister, G. Zhu, J. Pfeifer, and A. Bax, *J. Biomol. NMR* **6**(3), 277–293 (1995).